Mon. Not. R. Astron. Soc. **000**, 000–000 (0000) Printed 18 July 1996 (MN LaTeX style file v1.4)

Aperture Multipole Moments from Weak Gravitational Lensing

Peter Schneider and Matthias Bartelmann
Max-Planck-Institut für Astrophysik, Postfach 1523, D-85740 Garching, Germany

18 July 1996

ABSTRACT
The projected mass of a gravitational lens inside (circular) apertures can be derived from the measured shear inside an annulus which is caused by the tidal field of the deflecting mass distribution. Here we show that also the multipoles of the two-dimensional mass distribution can be derived from the shear in annuli. We derive several expressions for these mass multipole moments in terms of the shear, which allow large flexibility in the choice of a radial weight function. In contrast to determining multipole moments from weak-lensing mass reconstructions, this approach allows to quantify the signal-to-noise ratio of the multipole moments directly from the observed galaxy ellipticities, and thus to estimate the significance of the multipole detection. Radial weight functions can therefore be chosen such as to optimize the significance of the detection given an assumed radial mass profile. Application of our formulae to numerically simulated clusters demonstrates that the quadrupole moment of realistic cluster models can be detected with high signal-to-noise ratio S/N; in $\simeq 85$ per cent of the simulated cluster fields $S/N \gtrsim 3$. We also show that the shear inside a circular annulus determines multipole moments inside and outside the annulus. This is relevant for clusters whose central region is too bright to allow the observation of the shear of background galaxies, or which extend beyond the CCD. We also generalize the aperture mass equation to the case of 'radial' weight functions which are constant on arbitrarily-shaped curves which are not necessarily self-similar.

1 INTRODUCTION

As was shown by Kaiser & Squires (1993), the observable image distortion of high-redshift galaxies by an intervening mass concentration acting as a gravitational lens can be used to reconstruct the two-dimensional mass map of the deflector. The local mean image distortion provides an estimate for the local tidal gravitational field, from which the underlying surface mass density can be obtained. Since then, the original inversion method has been generalized in several ways (see, e.g., Schneider 1996a for a recent review and references). The mass maps obtained in this way are noisy, and the significance of individual features is not easily assessed. Kaiser (1995) proposed to use a measure for the mass convolved with a compensated top-hat filter. This so-called ζ-statistics, or aperture mass, has the advantage that the statistical properties of this mass estimate can be easily obtained from the observations. This statistics was then modified to allow for more general radial weight functions (Kaiser et al. 1994), and proposed by Schneider (1996b) as a means to search for 'dark' mass halos on wide-field images.

Recently, Wilson, Cole, & Frenk (1996) have investigated the possibility of studying the asymmetry of galaxy clusters with weak-lensing methods. As is well known (e.g., Richstone, Loeb, & Turner 1992; Bartelmann, Ehlers, & Schneider 1993), the amount of asymmetry in clusters depends quite strongly on the cosmological model, since it signifies the degree of relaxation, and thus age, of the clusters. High-density models predict a much later cluster formation epoch, and thus more asymmetric clusters, than low-density models of the universe. Wilson et al. (1996) applied the Kaiser & Squires (1993) cluster mass reconstruction algorithm to a sample of numerically generated cluster models and investigated the quadrupole moment of the *area* enclosed by a selected isodensity contour. Doing so, they showed that this measure indeed discriminates well between high- and low-Ω universes if applied to a fairly small number of massive clusters.

Here we derive mass multipole moments in circular apertures in terms of the shear in an annulus. As in the case of aperture masses, the chief advantage of aperture measures for the multipole moments is its direct relation to observable quantities, which allows to unambiguously quantify the accuracy, and thus the significance, of the result. Multipole moments can also be determined from mass maps derived from cluster mass reconstructions (e.g., Kaiser & Squires 1993; Seitz & Schneider 1995; Bartelmann et al. 1996; Wilson et al. 1996). Apart from being technically more involved, the inference in this case is indirect because multipoles are determined from the reconstructed mass maps rather than directly from the shear data, it does not allow to give simple error estimates, and it depends on artificial parameters like a smoothing length.

In contrast to the aperture mass, the weight functions (filters) do not need to be compensated. With two different methods, the aperture multipoles in terms of the shear field are derived in Sect. 2, leading to two apparently different expressions. It is shown in Appendix A that these two expressions are equivalent, and they can be suitably combined to allow for a large flexibility in the choice of the weight function. Several examples for this are presented. Alike the aperture mass, the mass multipoles inside a circle can be derived from the shear in an annulus outside that circle. In particular, as will be shown explicitly in Appendix B, the shear in a circular annulus is determined by the mass in this annulus, and the multipole moments of the mass inside and outside the annulus. We then investigate in Sect. 3 the signal-to-noise statistics of the aperture multipoles, using as a simple example a quasi-elliptical mass distribution. In Sect. 4 we present a preliminary analysis of the quadrupole moments of numerically generated cluster models to demonstrate the applicability of our method to realistic clusters. As discussed in Sect. 5, the application to a larger sample of cluster models drawn from different cosmological simulations provides an alternative approach to the discrimination between different cosmological scenarios.

The methods used for deriving the aperture multipoles are then used in Appendix C to generalize the aperture mass to weight functions which are constant on a set of nested arbitrarily-shaped curves which are not necessarily self-similar.

2 APERTURE MULTIPOLES

2.1 Definitions

Consider a mass distribution, e.g., a cluster of galaxies, at redshift $z_{\rm d}$, with surface mass density $\Sigma(\vec{x})$. The dimensionless surface mass density $\kappa(\vec{x})$ is defined as usual in gravitational lensing,

$$\kappa(\vec{x}) = \frac{\Sigma(\vec{x})}{\Sigma_{\rm cr}} \,, \tag{1}$$

with the critical density

$$\Sigma_{\rm cr} = \frac{c^2 D_{\rm s}}{4\pi G\, D_{\rm d}\, D_{\rm ds}} \,, \tag{2}$$

and the D's denote the angular-diameter distances between observer, deflector and source, and between deflector and source (for notation, see Schneider, Ehlers, & Falco 1992). For simplicity, we will provisionally assume that all faint galaxies are at the same redshift $z_{\rm s}$. The generalization to sources distributed in redshift will be discussed in Sect. 3.

We define the tensor of quadrupole moments of the two-dimensional mass distribution $\kappa(\vec{x})$ with respect to the point $\vec{x}_0$ as

$$Q_{ij} = \int {\rm d}^2x\; \kappa(\vec{x}+\vec{x}_0)\, w\left(|\vec{x}|\right)\, x_i\, x_j \,, \tag{3}$$

for $i,j \in \{1,2\}$, where $w(x)$ is a radial weight function. Combining the trace-free part of this tensor into a complex number $Q = Q_{11} - Q_{22} + 2{\rm i}Q_{12}$, this can be written as

$$Q = \int_0^\infty {\rm d}x\, x^3\, w(x) \int_0^{2\pi} {\rm d}\varphi\, {\rm e}^{2{\rm i}\varphi}\, \kappa(\vec{x}+\vec{x}_0) \,, \tag{4}$$

whereas the trace of Q_{ij} becomes

$$M := Q_{11} + Q_{22} = \int_0^\infty {\rm d}x\, x^3\, w(x) \int_0^{2\pi} {\rm d}\varphi\, \kappa(\vec{x}+\vec{x}_0) \,. \tag{5}$$

These equations are easily generalized for higher multipole orders. We define the complex $n^{\rm th}$-order multipole moment by

$$Q^{(n)} := \int_0^\infty {\rm d}x\, x^{n+1}\, w(x) \int_0^{2\pi} {\rm d}\varphi\, {\rm e}^{n{\rm i}\varphi} \kappa(\vec{x}+\vec{x}_0) \,, \tag{6}$$

and the 'mass moments'

$$M^{(n)} := \int_0^\infty {\rm d}x\, x^{n+1}\, w(x) \int_0^{2\pi} {\rm d}\varphi\, \kappa(\vec{x}+\vec{x}_0) \,. \tag{7}$$

Obviously, $Q^{(2)} \equiv Q$ and $M^{(2)} \equiv M$.

2.2 Multipole moments in terms of the shear

Let $\psi(\vec{x})$ denote the deflection potential, which is related to the surface mass density κ through the Poisson-like equation

$$\kappa = \frac{1}{2}\nabla^2\psi = \frac{1}{2}\left(\psi_{,11} + \psi_{,22}\right) \ , \tag{8}$$

where indices preceded by a comma denote partial derivatives. The two components of the local shear $\gamma(\vec{x}) = \gamma_1 + \mathrm{i}\gamma_2$ are then given by

$$\gamma_1 = \frac{1}{2}\left(\psi_{,11} - \psi_{,22}\right) \quad , \quad \gamma_2 = \psi_{,12} \ . \tag{9}$$

It was shown by Kaiser (1995) by suitably combining third-order derivatives of ψ that the gradient of κ can be written in terms of derivatives of the shear components as follows:

$$\nabla\kappa = \begin{pmatrix} \gamma_{1,1} + \gamma_{2,2} \\ \gamma_{2,1} - \gamma_{1,2} \end{pmatrix} \ . \tag{10}$$

This relation can now be used to express the multipole moments defined above in terms of the shear γ. Since the shear is directly observable from the distortion of the images of faint background galaxies (at least in the case of weak lensing, i.e., $\kappa \ll 1$), the multipole moments can be written directly in terms of observables.

For later convenience, we define the *tangential shear* $\gamma_{\mathrm{t}}(\vec{x};\vec{x}_0)$ *and the radial shear* $\gamma_{\mathrm{r}}(\vec{x};\vec{x}_0)$ *at position* $\vec{x} = x\,\mathrm{e}^{\mathrm{i}\varphi}$ *relative to position* $\vec{x}_0$ by

$$\begin{aligned} \gamma_{\mathrm{t}}(\vec{x};\vec{x}_0) &= -\left[\gamma_1\cos(2\varphi) + \gamma_2\sin(2\varphi)\right] = -\Re\left[\gamma(\vec{x}+\vec{x}_0)\,\mathrm{e}^{-2\mathrm{i}\varphi}\right] \ , \\ \gamma_{\mathrm{r}}(\vec{x};\vec{x}_0) &= -\left[\gamma_2\cos(2\varphi) - \gamma_1\sin(2\varphi)\right] = -\Im\left[\gamma(\vec{x}+\vec{x}_0)\,\mathrm{e}^{-2\mathrm{i}\varphi}\right] \ , \end{aligned} \tag{11}$$

where $\Re(z)$ and $\Im(z)$ denote the real and imaginary part of the complex number z.

2.2.1 First derivation

We integrate the φ-integral in (6) by parts to obtain

$$Q^{(n)} = \frac{\mathrm{i}}{n}\int_0^\infty \mathrm{d}x\, x^{n+1}\, w(x) \int_0^{2\pi} \mathrm{d}\varphi\, \mathrm{e}^{\mathrm{i}\,n\varphi}\, \frac{\partial\kappa}{\partial\varphi} \ . \tag{12}$$

The derivative of κ with respect to φ can be substituted after transforming (10) to polar coordinates. Subsequently, terms containing partial derivatives with respect to x and φ can be partially integrated with respect to x and φ, respectively. This leads to

$$Q^{(n)} \equiv Q_\varphi^{(n)} = \int_0^\infty \mathrm{d}x\, x^{n+1}\, w(x) \int_0^{2\pi} \mathrm{d}\varphi\, \mathrm{e}^{n\mathrm{i}\varphi}\, \gamma_{\mathrm{t}}(\vec{x};\vec{x}_0) + \frac{\mathrm{i}}{n}\int_0^\infty \mathrm{d}x\, \left[n x^{n+1} w(x) + x^{n+2} w'(x)\right] \int_0^{2\pi} \mathrm{d}\varphi\, \mathrm{e}^{n\mathrm{i}\varphi}\, \gamma_{\mathrm{r}}(\vec{x};\vec{x}_0) \ , \tag{13}$$

where $w'(x)$ is the derivative of $w(x)$, and $w(x)$ has to be continuous and piecewise differentiable. In order to get rid of the boundary terms in the partial integrations leading to (13), $w(x)$ has to satisfy the conditions

$$|\gamma|\, x^{n+2}\, w(x) \to 0 \quad \text{for} \quad x \to 0 \quad \text{and} \quad x \to \infty \ . \tag{14}$$

2.2.2 Second derivation

Alternatively, we can integrate (6) by parts with respect to x and find

$$Q^{(n)} = -\int_0^\infty \mathrm{d}x\, x\, W(x) \int_0^{2\pi} \mathrm{d}\varphi\, \mathrm{e}^{n\mathrm{i}\varphi}\, \frac{\partial\kappa}{\partial x} \ , \tag{15}$$

where $W(x)$ is related to the weight function $w(x)$ by

$$x\, W(x) = \int_0^x \mathrm{d}y\; y^{n+1}\, w(y) \ . \tag{16}$$

Substituting into (15) the radial derivative of κ from (10) transformed to polar coordinates, we obtain

$$Q^{(n)} \equiv Q_x^{(n)} = \int_0^\infty \mathrm{d}x\, \left[2W(x) - x^{n+1}\, w(x)\right] \int_0^{2\pi} \mathrm{d}\varphi\, \mathrm{e}^{n\mathrm{i}\varphi}\, \gamma_{\mathrm{t}}(\vec{x};\vec{x}_0) - \mathrm{i}\, n \int_0^\infty \mathrm{d}x\, W(x) \int_0^{2\pi} \mathrm{d}\varphi\, \mathrm{e}^{n\mathrm{i}\varphi}\, \gamma_{\mathrm{r}}(\vec{x};\vec{x}_0) \ . \tag{17}$$

The boundary terms in the partial integration leading to (15) vanish if $W(x)$ satisfies

$$x\,W(x)\,\kappa \to 0 \quad \text{for} \quad x \to 0 \quad \text{and} \quad x \to \infty\,. \tag{18}$$

We have thus derived two expressions for $Q^{(n)}$ which are of quite different form. We prove their equivalence in Appendix A, using the fact that the two components of the shear are not mutually independent, but related via the underlying deflection potential. Another way to see the equivalence is to note that the curl of the vector field on the right-hand-side of (10) must vanish, which is a condition not used in the derivation of either (13) or (17).

After a sequence of partial integrations similar to those used before, the mass moments (7) become

$$M^{(n)} = \int_0^\infty \mathrm{d}x\, \left[2W(x) - x^{n+1}\,w(x)\right] \int_0^{2\pi} \mathrm{d}\varphi\, \gamma_{\rm t}(\vec{x};\vec{x}_0)\,, \tag{19}$$

which is the mass aperture equation of Kaiser et al. (1994; see also Schneider 1996b).

2.3 Aperture multipole measures

The fact that we have two different, but equivalent, expressions for the multipole moments $Q^{(n)}$ provides some freedom in choosing the weight functions $w(x)$ and $W(x)$ suitably. Recall the situation for the aperture mass measures as discussed in Schneider (1996b). There, from shear data in a ring with $x \in [\nu R, R]$ with $\nu < 1$, the aperture mass measure $m \equiv M^{(0)}$ can be determined, provided the weight function $w(x)$ satisfies $\int \mathrm{d}x\, x\, w(x) = 0$. This condition arises because the shear determines the surface mass density only up to an additive constant, and the normalization condition on w guarantees that this unknown additive constant drops out of the aperture mass. As an aside, we generalize the aperture mass formula to arbitrarily shaped apertures in Appendix C.

Similarly, we assume here that shear data are given in the ring $x \in [\nu R, R]$, where in practice the outer radius R is determined by the size of the CCD, and an inner radial distance from the cluster center may be required if the cluster contains bright central galaxies which outshine the images of faint background galaxies. Then, $Q_\varphi^{(n)}$ is a *local* estimator for $Q^{(n)}$, in the sense that if the weight function $w(x)$ is nonzero only in a specified radial interval, the estimate $Q_\varphi^{(n)}$ requires shear data only from that interval. However, it should be noted that the boundary terms in the integrations by parts with respect to x leading to (13) vanish only if $w(x) = 0$ at the boundaries of the interval.

In contrast to $Q_\varphi^{(n)}$, $Q_x^{(n)}$ is a *non-local* estimate of $Q^{(n)}$, for it requires shear data from outside the interval, unless $W(x)$ also vanishes outside the specified interval. It follows from (16) that $W(x) = 0$ outside an interval imposes integral constraints on $w(x)$, whereas $w(x)$ is an arbitrary function in the estimator $Q_\varphi^{(n)}$ (except that it has to vanish at the interval boundaries).

To simplify notation in the remainder of the paper, we introduce the abbreviations

$$g_{\rm t}(x) := \int_0^{2\pi} \mathrm{d}\varphi\, \mathrm{e}^{n\mathrm{i}\varphi}\, \gamma_{\rm t}(\vec{x};\vec{x}_0) \quad , \quad g_{\rm r}(x) := \mathrm{i}\int_0^{2\pi} \mathrm{d}\varphi\, \mathrm{e}^{n\mathrm{i}\varphi}\, \gamma_{\rm r}(\vec{x};\vec{x}_0)\,. \tag{20}$$

2.3.1 Local estimate of $Q^{(n)}$

Let $w_1(x)$ be a weight function which vanishes outside the interval $x \in [\nu R, R]$, and let $w_1(\nu R) = w_1(R) = 0$. Then, the *local* estimate of the multipole moment $Q^{(n)}$ corresponding to this weight function is given by

$$Q_1^{(n)} = \int_{\nu R}^R \mathrm{d}x\, x^{n+1}\, w_1(x)\, g_{\rm t}(x) + \frac{1}{n}\int_{\nu R}^R \mathrm{d}x\, x^{n+1}\left[n w_1(x) + x w_1'(x)\right]\, g_{\rm r}(x)\,. \tag{21}$$

This equation is applicable to the case when multipole information is to be determined on the circle $x \le R$ (i.e. $\nu = 0$) or on the ring $\nu R \le x \le R$ from shear data measured in the same regions.

2.3.2 Non-local estimates of $Q^{(n)}$

We now want to address the following question. Suppose data are available within the radial interval $\nu R \le x \le R$ only, can we estimate the multipole moments for $x < \nu R$ and $x > R$? Since $Q_\varphi^{(n)}$ and $Q_x^{(n)}$ are equivalent estimates of $Q^{(n)}$, one can combine the two with weights α and $(1-\alpha)$, respectively, to obtain

$$\begin{aligned} Q^{(n)} = \alpha Q_\varphi^{(n)} + (1-\alpha) Q_x^{(n)} &= \int_0^\infty \mathrm{d}x\, \left[(2\alpha-1)x^{n+1}\,w(x) + 2(1-\alpha)\,W(x)\right]\, g_{\rm t}(x) \\ &+ \int_0^\infty \mathrm{d}x\, \left[\alpha x^{n+1}\,w(x) + \frac{\alpha}{n}x^{n+2}\,w'(x) - n(1-\alpha)W(x)\right]\, g_{\rm r}(x)\,. \end{aligned} \tag{22}$$

In the light of this equation, we ask whether we can choose the weight α and the weight function $w(x)$ such that the integrands in (22) vanish outside $[\nu R, R]$, but with $w(x)$ not identically zero outside that interval. If that were possible, we could deduce some information on the multipoles of the deflector in those regions where no shear information is available.

The requirement that the brackets in the two integrals of (22) vanish leads to two solutions for the weight function $w(x)$ and the corresponding weights α,

$$w_+(x) = \text{const.} \quad \text{with} \quad \alpha_+ = \frac{n}{2(n+1)} \quad ; \quad w_-(x) \propto x^{-2n} \quad \text{with} \quad \alpha_- = \frac{n}{2(n-1)} \; , \tag{23}$$

where the latter is valid only for $n \ge 3$.

We first consider the multipole moment within the circle $x \le \nu R$, i.e. interior to the region of the data. Thus, we search for a weight function $w_2(x)$ which vanishes for $x > R$, but which is finite for $x < \nu R$. Hence, $w_2(x)$ must be of the form (23) for $x < \nu R$. Since $w_-(x)$ does not satisfy the conditions (14) and (18), $w_2(x) = \text{const.}$ for $x \le \nu R$, and we choose $w_2(x) = 1$ for $x \le \nu R$ without loss of generality. In order for $W_2(x)$ to vanish for $x > R$, we further require

$$\int_0^R \mathrm{d}x \; x^{n+1} \, w_2(x) = 0 \; . \tag{24}$$

Hence, the 'internal' multipole moment $Q_2^{(n)}$ corresponding to the weight function w_2 with the aforementioned properties becomes

$$Q_2^{(n)} = \frac{1}{2(1+n)} \int_{\nu R}^R \mathrm{d}x \left\{ \left[(4+2n) W_2(x) - 2x^{n+1} w_2(x) \right] g_\mathrm{t}(x) + \left[n x^{n+1} w_2(x) + x^{n+2} w_2'(x) - (2+n) n W_2(x) \right] g_\mathrm{r}(x) \right\} , \tag{25}$$

where we have inserted the weight α_+ from (23).

Next, we consider the multipole moment outside the circle $x = \nu R$, i.e. exterior to the region of the data. We therefore require a weight function which vanishes for $x < \nu R$, but is non-zero for $x > R$. This weight function, called $w_3(x)$, needs to satisfy the condition – see (14) and (18) –

$$\int_{\nu R}^{\infty} \mathrm{d}x \, x^{n+1} \, w_3(x) = 0 \; , \tag{26}$$

and if it behaves like $w(x) \propto x^{-2n}$ for $x > R$, then the multipole moments become, for $n \ge 3$,

$$Q_3^{(n)} = \frac{1}{2(n-1)} \int_{\nu R}^R \mathrm{d}x \left\{ \left[2x^{n+1} w_3(x) + (2n-4) W_3(x) \right] g_\mathrm{t}(x) + \left[n x^{n+1} w_3(x) + x^{n+2} w_3' - n(n-2) W_3(x) \right] g_\mathrm{r}(x) \right\} . \tag{27}$$

This equation is not valid for $n = 2$ because then $w \propto x^{-4}$ for $x > R$, and $W(x)$ becomes logarithmic. We have not been able to find a relation for the *external* quadrupole moment. We show in Appendix B that the shear in the annulus caused by matter not in the annulus is completely determined by the set of multipole moments of the matter inside the annulus (i.e., at $x < \nu R$) and the multipoles of order $n \ge 2$ of the matter outside the annulus.

Of course, the different local and non-local expressions for the mass multipoles can be combined appropriately. As a simple example, consider the case that we want to infer $Q^{(n)}$ for $0 \le x \le R$. We then need to combine the *internal* multipole moment (25) with the *local* multipole moment (21). Thus suppose we have a weight function $w(x)$ which is constant for $0 \le x \le \nu R$ and smoothly falls off to zero for $x \to R$. Then, $w(x)$ can be decomposed into $w(x) = w_1(x) + w_2(x)$, where $w_1(x)$ vanishes for $x < \nu R$ and $x > R$, and $w_2(x)$ is constant for $x < \nu R$, vanishes for $x > R$, and satisfies the constraint (24). Since the aperture multipoles $Q^{(n)}$ are linear in the weight function $w(x)$, different expressions for $Q^{(n)}$ can be appropriately superposed. To use a weight function of the form just discussed, one would have to insert $w_1(x)$ into (21) to obtain $Q_1^{(n)}$ and $w_2(x) = w(x) - w_1(x)$ into (25) to obtain $Q_2^{(n)}$, and the multipole moment would be the sum of the two, $Q^{(n)} = Q_1^{(n)} + Q_2^{(n)}$.

3 MULTIPOLE SIGNAL-TO-NOISE RATIO

The aperture multipole moments calculated in the previous section are all of the form

$$Q^{(n)} = \int_{\nu R}^R \mathrm{d}x \; \left[b_\mathrm{t}(x) \, g_\mathrm{t}(x) + b_\mathrm{r}(x) \, g_\mathrm{r}(x) \right] \; . \tag{28}$$

With (20), we can rewrite (28) as

$$Q^{(n)}(\vec{x}_0) = \int \mathrm{d}^2 x \; \mathrm{e}^{n\mathrm{i}\varphi} \left(\frac{b_\mathrm{t}(x)}{x} \gamma_\mathrm{t}(\vec{x}; \vec{x}_0) + \mathrm{i} \frac{b_\mathrm{r}(x)}{x} \gamma_\mathrm{r}(\vec{x}; \vec{x}_0) \right) \; , \tag{29}$$

where we have re-introduced the explicit dependence on the center $\vec{x}_0$ of the aperture.

In order to apply this equation to data, one needs to approximate the integral by a sum over individual image ellipticities. Let ϵ_i be the complex ellipticity of the i-th galaxy image at position $\vec{x}_i$. As in Schneider (1996b), the modulus of the ellipticity for an elliptical image is defined as $|\epsilon| = (1-r)/(1+r)$, where r is the axis ratio, and the phase is twice the angle enclosed by the major axis and the positive x_1-axis. In the case of weak lensing, $\kappa \ll 1$, ϵ_i is an unbiased estimator for the shear $\gamma(\vec{x}_i)$. Since then γ depends linearly on the distance ratio $D_{\rm ds}/D_{\rm s}$, the following relations are valid in the case of weak lensing for a redshift distribution of the sources, with $D_{\rm ds}/D_{\rm s}$ replaced by $\langle D_{\rm ds}/D_{\rm s}\rangle$, the average over all galaxies used. Since we will mainly be dealing with those regions of the lenses where $\kappa \ll 1$ (e.g., by choosing the aperture radii appropriately), we write the discretized version of (29) as

$$Q^{(n)}(\vec{x}_0) = \frac{1}{\bar{n}} \sum_{i=1}^{N} {\rm e}^{n{\rm i}\vartheta_i} \left(\frac{b_{\rm t}(y_i)}{y_i} \epsilon_{{\rm t}i} + {\rm i} \frac{b_{\rm r}(y_i)}{y_i} \epsilon_{{\rm r}i} \right) , \tag{30}$$

where $\bar{n}$ is the number density of galaxy images in the annulus. We have introduced polar coordinates (y_i, ϑ_i) such that

$$\vec{x}_i = y_i \begin{pmatrix} \cos\vartheta_i \\ \sin\vartheta_i \end{pmatrix} + \vec{x}_0 , \tag{31}$$

and the tangential and radial components of the image ellipticity are defined in analogy with (11) as

$$\epsilon_{{\rm t}i} = -\Re\left(\epsilon_i\, {\rm e}^{-2{\rm i}\vartheta_i}\right) \quad ; \quad \epsilon_{{\rm r}i} = -\Im\left(\epsilon_i\, {\rm e}^{-2{\rm i}\vartheta_i}\right) . \tag{32}$$

In the *absence* of a lens, the expectation value of $Q^{(n)}$ is zero, and its dispersion is

$$\left(\sigma_{\rm d}^{(n)}\right)^2 := \left\langle |Q^{(n)}|^2 \right\rangle = \frac{1}{\bar{n}^2} \frac{\sigma_\epsilon^2}{2} \sum_{i=1}^{N} \left[\left(\frac{b_{\rm t}(y_i)}{y_i}\right)^2 + \left(\frac{b_{\rm r}(y_i)}{y_i}\right)^2 \right] , \tag{33}$$

where we have used that, in the absence of lensing,

$$\langle \epsilon_{{\rm t}i}\epsilon_{{\rm t}j}\rangle = \langle \epsilon_{{\rm r}i}\epsilon_{{\rm r}j}\rangle = \delta_{ij}\frac{\sigma_\epsilon^2}{2} \quad ; \quad \langle \epsilon_{{\rm t}i}\epsilon_{{\rm r}j}\rangle = 0 , \tag{34}$$

and σ_ϵ is the dispersion of the intrinsic source ellipticity. The ensemble average of the dispersion is

$$\left(\sigma_{\rm c}^{(n)}\right)^2 = \left[\prod_{k=1}^{N} \int_{\nu R}^{R} \frac{2x_k\,{\rm d}x_k}{(1-\nu^2)R^2} \right] \left(\sigma_{\rm d}^{(n)}\right)^2 = \frac{\pi\sigma_\epsilon^2}{\bar{n}} \int_{\nu R}^{R} {\rm d}y\, \left(\frac{b_{\rm t}^2(y) + b_{\rm r}^2(y)}{y} \right) . \tag{35}$$

We can therefore obtain an approximation for the signal-to-noise ratio of the multipole moments,

$$S_{\rm c}^{(n)} = \frac{|Q^{(n)}|}{\sigma_{\rm c}^{(n)}} . \tag{36}$$

To obtain an estimate for the expected signal-to-noise ratio of the quadrupole moment of an elliptical mass distribution, we consider a singular isothermal ellipsoid, with surface-density distribution

$$\kappa(\vec{x}) = \frac{x_{\rm E}}{2\sqrt{(1-\eta)^2 x_1^2 + (1+\eta)^2 x_2^2}} . \tag{37}$$

It has an axis ratio of $r = (1-\eta)/(1+\eta)$, and $x_{\rm E}$ is the characteristic angular scale, which we choose as the Einstein radius of the corresponding singular isothermal sphere with velocity dispersion σ_v,

$$x_{\rm E} = 4\pi \left(\frac{\sigma_v}{c}\right)^2 \left\langle \frac{D_{\rm ds}}{D_{\rm s}} \right\rangle . \tag{38}$$

For this mass distribution, the quadrupole moment (4) becomes

$$Q^{(2)} = \frac{x_{\rm E}\, C(\eta)}{2} \int {\rm d}x\, x^{2n}\, w(x) , \tag{39}$$

where, for moderately small η, $C(\eta) = \pi\eta + \mathcal{O}(\eta^3)$. If we choose (21) for the determination of the quadrupole moment, the signal-to-noise ratio (36) reads

$$S_{\rm c}^{(2)} = \frac{C(\eta)\, x_{\rm E}\sqrt{\bar{n}}}{2\sqrt{\pi}\sigma_\epsilon} \frac{\int {\rm d}x\; x^2\, w(x)}{\sqrt{\int {\rm d}x\, x^5\, (2w^2 + xww' + x^2 w'^2/4)}} . \tag{40}$$

One can now try to find a weight function which maximizes $S_{\rm c}$ for the mass distribution under consideration. From the Cauchy-Schwarz inequality, it is easy to find that the optimized weight function is $w(x) \propto x^{-3}$. If this is inserted into (40), one sees that the integration has to be terminated at both ends, say at $x_{\rm min}$ and $x_{\rm max}$. We then find

$$S_{\rm c}^{(2)} = \frac{C(\eta)\, x_{\rm E}\, \sqrt{\bar{n}}}{\sqrt{5\pi}\sigma_\epsilon} \sqrt{\ln(x_{\rm max}/x_{\rm min})} \approx 4.5 \left(\frac{\eta}{0.2}\right) \left(\frac{\sigma_\epsilon}{0.2}\right)^{-1} \left(\frac{\bar{n}}{30\,{\rm arcmin}^{-2}}\right)^{1/2} \left(\frac{\sigma_v}{1000\,{\rm km\,s}^{-1}}\right)^2 \left\langle \frac{D_{\rm ds}}{D_{\rm s}} \right\rangle , \tag{41}$$

where is the second step we assumed that $(x_{\rm max}/x_{\rm min}) \sim 10$, and we used the approximation for $C(\eta)$ as given above.

The optimal weight function cannot be simply chosen as x^{-3}, since we have to satisfy (14). For the simulations presented below we therefore choose a weight function which behaves approximately like x^{-3} (and, for higher multipole moments, like $x^{-(n+1)}$), but with appropriate behaviour at $x = \nu R = 0$ and $x = R$,

$$w(x) = \frac{1}{x^{n+1} + x_{\rm min}^{n+1}} - \frac{1}{R^{n+1} + x_{\rm min}^{n+1}} + \frac{(n+1)R^n(x-R)}{\left(R^{n+1} + x_{\rm min}^{n+1}\right)^2} \; . \tag{42}$$

Using this weight function, we have made simulations by assuming a mass distribution of the form

$$\kappa(\vec{x}) = \frac{x_{\rm E}}{2\left(1-\eta'^2\right)^2} \left[2\left(1+\eta'^2\right)x_{\rm c}^2 + |\vec{x}|^2\right] \left[x_{\rm c}^2 + \frac{x_1^2}{(1-\eta')^2} + \frac{x_2^2}{(1+\eta')^2}\right]^{-3/2} , \tag{43}$$

which corresponds to an elliptical deflection potential of the form

$$\psi = x_{\rm E} \left(x_{\rm c}^2 + \frac{x_1^2}{(1-\eta')^2} + \frac{x_2^2}{(1+\eta')^2}\right)^{1/2} , \tag{44}$$

with axis ratio $(1-\eta')/(1+\eta')$. In the limit of vanishing ellipticity, $\eta' = 0$, and zero core size, $x_{\rm c} = 0$, (43) becomes the mass distribution of an isothermal sphere, with $x_{\rm E}$ given by (38). For $|\vec{x}| \gg x_{\rm c}$, the isodensity contours have an axis ratio of $(1-\eta')^3/(1+\eta')^3$, which is 0.74 (0.55, 0.40) for $\eta' = 0.05$ (0.1, 0.15). Galaxies with $\langle D_{\rm ds}/D_{\rm s}\rangle = 0.7$ and a surface density of $30\,{\rm arcmin}^{-2}$ were distributed and sheared according to the mass distribution (43). The galaxies were assumed to have a Gaussian ellipticity distribution with $\sigma_\epsilon = 0.2$. In Fig. 1 we show the result of one such simulation, with $\sigma_v = 1000\,{\rm km\,s}^{-1}$, $x_{\rm min} = 0.1R$, $R = 5'$, $x_{\rm c} = 1.5x_{\rm E}$ (i.e., the lens is subcritical), and four different values of η'. We have plotted there the cumulative probability for the signal-to-noise ratio

$$S = \frac{|Q^{(2)}|}{\sigma_{\rm d}^{(2)}} , \tag{45}$$

as given by (30) and (33). As can be seen from Fig. 1, the typical signal-to-noise ratio of the quadrupole moment for a lens with $\eta' \gtrsim 0.1$ is considerably larger than the median of the S-distribution for a spherical lens. That means that for these mass distributions the quadrupole moment can be detected at a statistically significant level, whereas for the distribution with $\eta' = 0.05$, there is a considerable overlap between the probability distribution of the elliptical lens and the corresponding spherical mass distribution.

4 APPLICATION TO NUMERICAL CLUSTER SIMULATIONS

Having seen in the previous section that the aperture quadrupole from gravitational shear can significantly be detected for moderately elliptical idealized lens mass distributions, we proceed here to study the aperture quadrupole for numerically simulated clusters. From a large sample of gas-dynamical cluster simulations performed within the standard CDM cosmogony (for a detailed description of the sample see Bartelmann & Steinmetz 1996), we select a subsample of 13 clusters, all at redshift $z_{\rm d} = 0.3$. Since we can project them along three independent spatial directions, we have in total 39 surface-mass distributions from these clusters. Assuming sources at redshift $z_{\rm s} = 1$, their maximum convergence values range between $0.27 \le \kappa_{\rm max} \le 1.40$, with the median at $\kappa_{\rm max} \simeq 0.73$, and one third of them are critical lenses, i.e., they produce critical curves.

For each of the 39 simulated cluster fields, we simulate 200 source galaxy distributions with a galaxy density of $40\,{\rm arcmin}^{-2}$. Since the fields have a side length of $5'$, the average number of source galaxies per cluster field is 10^3. Their positions are distributed randomly, and they are assigned an ellipticity drawn from a Gaussian distribution with dispersion $\sigma_\epsilon = 0.15$.

We then determine from each simulation the aperture quadrupole estimate $Q^{(2)}$ according to (30) and the aperture signal-to-noise ratio according to (45), using a weight function $w(x)$ of the form given in (42). There, $R = 2\overset{'}{.}5$, and we choose $x_{\rm min} = 1'$. Since $w(x)$ has the dimension $({\rm length})^{-3}$, the quadrupole moment has the dimension (length), and we give it in units of arc minutes in the following figures.

Figure 2 shows for each cluster in the sample the fraction of the 200 lensing simulations for which the aperture quadrupole is determined with a signal-to-noise ratio (S/N) larger than some threshold $(S/N)_0$, as a function of the modulus of the true cluster quadrupole as defined in (4). The difference between the four panels in the figure is the signal-to-noise threshold $(S/N)_0$. In panels (a,b,c,d) we have chosen, respectively, $(S/N)_0 = \{2, 3, 5, 10\}$. All panels show that the significance of the aperture quadrupole measurement increases with increasing intrinsic quadrupole $|Q^{(2)}_{\rm true}|$, as expected. While the aperture quadrupole can be determined with $(S/N) > 2$ for all clusters with $|Q^{(2)}_{\rm true}| \gtrsim 0\overset{'}{.}05$ (panel a), $|Q^{(2)}_{\rm true} \gtrsim 0\overset{'}{.}1$ is required for $(S/N) > 5$ (panel c), and only a small fraction of clusters allows to determine the aperture quadrupole with $(S/N) > 10$ (panel d). For further information, the different symbols denote the maximum convergence value $\kappa_{\rm max}$ of the clusters. We use

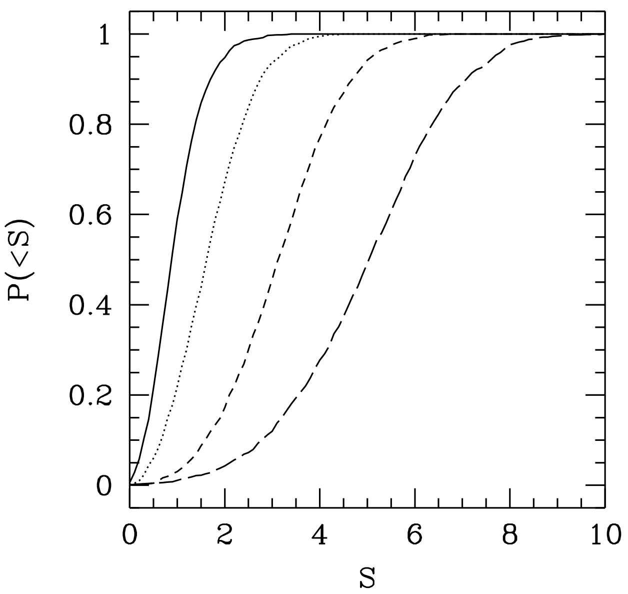

Figure 1. The cumulative probability distribution $P(< S)$ for a signal-to-noise ratio, as defined in (45), being greater than S. For these simulations, a galaxy density of $30/\mathrm{arcmin}^2$ has been assumed, with an intrinsic ellipticity dispersion of $\sigma_\epsilon = 0.2$ and a mean distance ratio $\langle D_{\rm ds}/D_{\rm s}\rangle = 0.7$. For the lens, a mass distribution of the form (43) was assumed, with $\sigma_v = 1000\,\mathrm{km\,s^{-1}}$, core size $x_{\rm c} = 1.5 x_{\rm E}$, and four different ellipticity parameters $\eta' = 0$ (solid curve), 0.05 (dotted curve), 0.1 (short-dashed curve) and 0.15 (long-dashed curve)

triangles (squares, hexagons) for $\kappa_{\rm max} < 0.7$ ($0.7 \le \kappa_{\rm max} < 0.83$, $0.83 \le \kappa_{\rm max}$), where the intervals are chosen such that they encompass one third of the cluster sample each. The distribution of these symbols along the curves shows that the aperture quadrupole can only be determined significantly if $\kappa_{\rm max}$ is not too small.

While the shear γ enters into the formula for the aperture multipoles (13), the distortion of background objects measures the reduced shear, which is a combination of shear and convergence, $g \equiv \gamma(1-\kappa)^{-1}$, rather than the shear. In the case of weak lensing, $g \approx \gamma$, and then the measured galaxy ellipticities provide an unbiased estimate for γ. If lensing is not weak, however, the observed aperture multipole (30) is a biased estimate of the true multipole. Since $\kappa > 0$, $Q^{(n)}$ as determined from (30) overestimates the true aperture multipole. This is demonstrated in Fig. 3, where we show the distribution of aperture quadrupole measurements relative to the true aperture quadrupole for three clusters with approximately equal true quadrupole, but with different maximum convergence values $\kappa_{\rm max}$.

As a test, we have verified that the systematic bias in the quadrupole measurement disappears when we distort the galaxy images with the shear alone rather than with the reduced shear. Apart from the bias, the distribution of points in Fig. 3 shows that the scatter in the quadrupole measurements is fairly low.

5 DISCUSSION

In this paper we have investigated the possibility to derive multipole moments of the projected mass distribution of clusters with weak-lensing techniques. Following the same ideas underlying the aperture mass measures (Kaiser 1995, Kaiser et al. 1994, Schneider 1996b), we have derived several expressions for the mass multipoles of clusters in terms of the shear distribution in a circle or an annulus around the cluster center. The shear distribution is observationally accessible through the ellipticities of faint background galaxies. In contrast to the aperture masses, the weight functions used for the multipoles do not need to be of zero total weight, because the additive constant in the mass reconstruction arising from the mass-sheet degeneracy is irrelevant for multipoles.

Our different expressions for the multipole moments can be adapted to a variety of observational situations:

– Expression (21) permits to determine the multipole in a circle or a ring from data given in the same region.
– Expression (25) allows to determine the multipole inside a circle from the shear data in an annulus which excludes the central region of the circle. This is relevant in cases when the central part of a cluster is dominated by bright cluster galaxies which outshine the faint background galaxies.

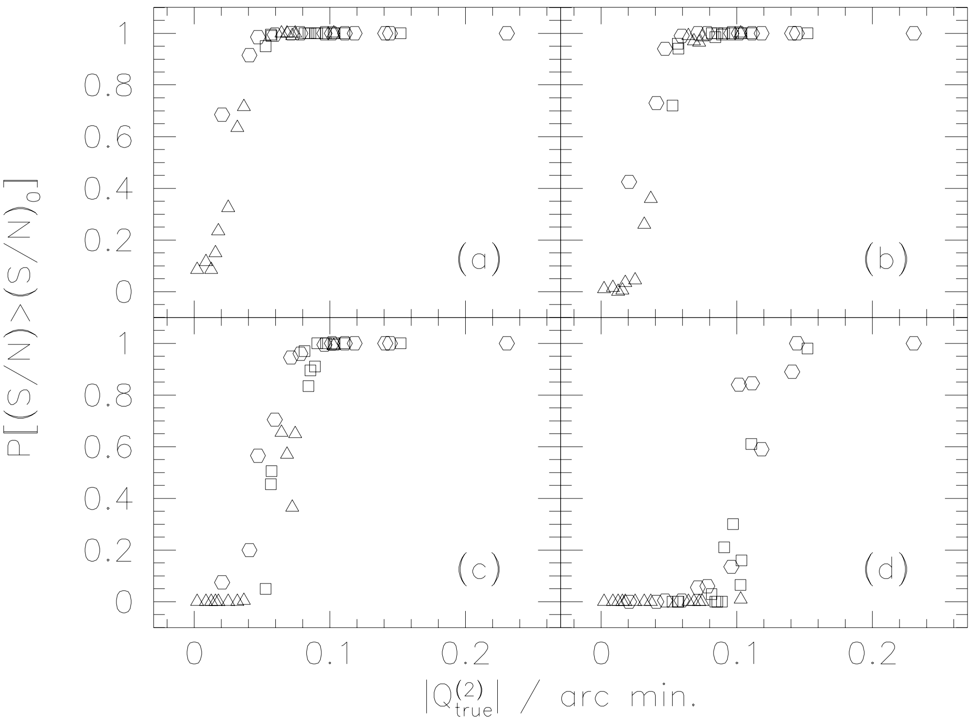

Figure 2. For each cluster in the sample with intrinsic quadrupole $|Q^{(2)}_{\rm true}|$ as defined in (4), the fraction of the 200 lensing simulations is shown for which the aperture quadrupole is determined with signal-to-noise ratio (S/N) larger than some limit $(S/N)_0$, where $(S/N)_0 = \{2, 3, 5, 10\}$ in panels (a,b,c,d), respectively. The triangles (squares, hexagons) distinguish between clusters with low (medium, high) maximum convergence $\kappa_{\rm max}$ (see text for details). The curves show that the aperture quadrupole can be determined with $(S/N) > 2$ for all clusters with $|Q^{(2)}_{\rm true}| \gtrsim 0\overset{\prime}{.}05$ and with $(S/N) > 5$ for all clusters with $|Q^{(2)}_{\rm true}| \gtrsim 0\overset{\prime}{.}1$, while only few clusters allow to determine the aperture quadrupole with $(S/N) > 10$.

– Expression (27) yields the multipole in a ring as before, but also outside the region where data are given. Hence, the multipole of a cluster can be determined even if the shear data do not cover the entire cluster.
– As discussed at the end of Sect. 2, these different expressions can be appropriately combined to match specific observational circumstances.

Analytic estimates and numerical experiments using simulated cluster mass distributions demonstrate that the quadrupole of massive clusters can be detected in a statistically significant way. As an aside, we have generalized the mass aperture relation to apertures of arbitrary shape, both for self-similar curves of constant weight (see also Squires & Kaiser 1996) and for arbitrary curves of constant weight.

The weight function $w(x)$ used in our numerical studies might not be the most appropriate choice. In particular, this weight function, when applied to the multipole formula (13), uses shear information from the entire circle $|\vec{x}| \le R$ and thus does not punch out a possible region of strong lensing in the clusters. Therefore, the measured image ellipticities are not an unbiased estimator of the shear in the inner part of the cluster, which systematically biases the aperture quadrupole moments high, as seen in Fig. 3. However, as explained at the end of Sect. 2, one can construct weight functions which avoid this problem and which still can be optimized for the detection of multipole moments of quasi-isothermal mass distributions.

Whereas our numerical results on clusters drawn from gas-dynamical large-scale structure simulations are encouraging and give us faith in the usefulness of the aperture multipole measures, they should be considered as a preliminary application only. The cosmological application of our new approach to quantifying the asymmetry of cluster mass distributions will require the generation of a sample of clusters simulated in different cosmological models. The comparison of the aperture multipole moments of clusters formed in different cosmologies will then show whether they are sufficiently powerful indicators of the cosmic density parameter Ω, and how our new method compares with the one suggested by Wilson et al. (1996). To compare clusters drawn from different cosmological simulations, not the quadrupole moments themselves should be compared because they depend on both the clusters mass (or velocity dispersion) and the degree of asymmetry, but normalized quadrupole moments. As such, the ratio of the quadrupole moment and the aperture mass seems to be an appropriate dimensionless

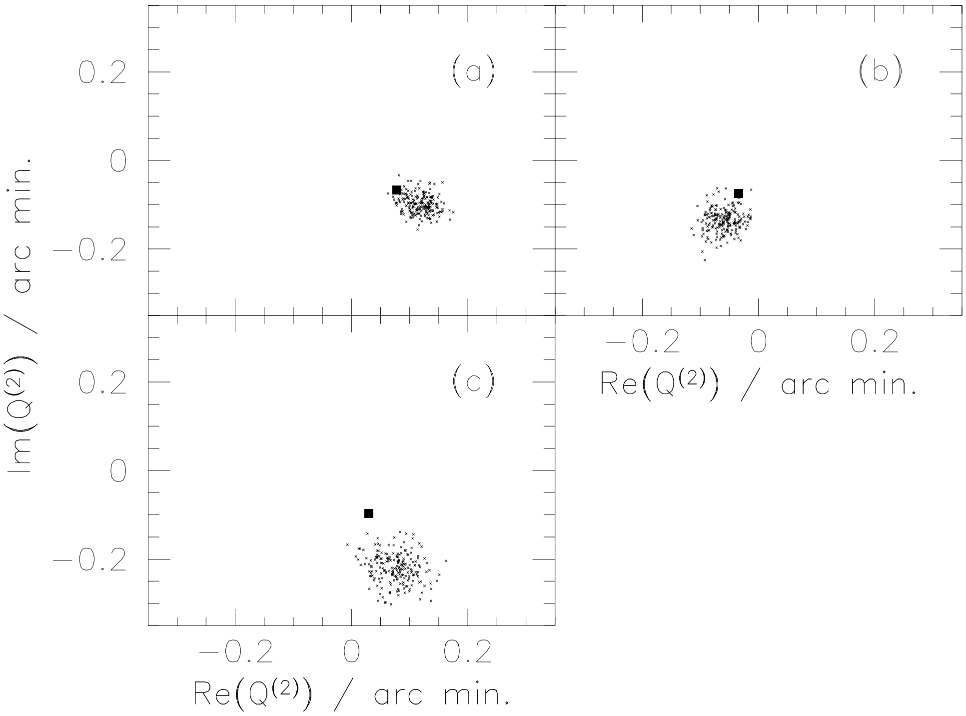

Figure 3. Distribution of aperture quadrupole estimates as obtained from (30) with simulated galaxy ellipticities (crosses), together with the true aperture quadrupole (filled squares), for three cluster models with approximately equal true quadrupole but different maximum convergence values $\kappa_{\rm max}$. In panels (a,b,c), $\kappa_{\rm max}=\{0.6,0.7,1.0\}$. The figure shows that the measured aperture quadrupole overestimates the true one because image ellipticities measure $\gamma(1-\kappa)^{-1}>\gamma$ rather than γ only.

measure of the degree of asphericity of a cluster. A detailed study of these issues, together with a comparison with the Wilson et al. method, will be the subject of a forthcoming study.

APPENDIX A: EQUIVALENCE OF $Q_\varphi^{(N)}(X)$ AND $Q_X^{(N)}(X)$

We will now explicitly show the equivalence of (13) and (17), starting from a general multipole expansion of the deflection potential. Choosing coordinates such that $\vec x_0=\vec 0$, we can write

$$\psi(\vec x)=\sum_{m=0}^{\infty} f_m(x)\,\cos(m\varphi+\varphi_m)\;; \tag{A1}$$

the function $f_m(x)$ are assumed to have continuous second derivatives. Using (8), (9), and (11), we can then write γ_1, γ_2, and κ, and hence also $\gamma_{\rm t}$, and $\gamma_{\rm r}$ in terms of the functions $f_m(x)$,

$$\begin{aligned}\gamma_{\rm t} &= -\frac{1}{2}\sum_{m=0}^{\infty}\cos(m\varphi+\varphi_m)\left(f_m''(x)-\frac{f_m'(x)}{x}+m^2\frac{f_m(x)}{x^2}\right)\;,\\ \gamma_{\rm r} &= \sum_{m=0}^{\infty} m\,\sin(m\varphi+\varphi_m)\left(\frac{f_m'(x)}{x}-\frac{f_m(x)}{x^2}\right)\;.\end{aligned} \tag{A2}$$

Using further the relations

$$\int_0^{2\pi}{\rm d}\varphi\,{\rm e}^{n{\rm i}\varphi}\,\cos(m\varphi+\varphi_m)=\pi\,{\rm e}^{-{\rm i}\varphi_m}\,\delta_{mn}\quad,\quad\int_0^{2\pi}{\rm d}\varphi\,{\rm e}^{n{\rm i}\varphi}\,\sin(m\varphi+\varphi_m)={\rm i}\pi\,{\rm e}^{-{\rm i}\varphi_m}\,\delta_{mn}\;, \tag{A3}$$

we find from (6) and (8) that

$$Q^{(n)} = \frac{\pi}{2}\,\mathrm{e}^{-\mathrm{i}\varphi_n}\int_0^\infty \mathrm{d}x\,x^{n+1}\,w(x)\,\left(f_n''(x)+\frac{f_n'(x)}{x}-n^2\frac{f_n(x)}{x^2}\right)\ . \tag{A4}$$

From (13), we find with the same procedure

$$\begin{aligned} Q^{(n)}_\varphi = \frac{\pi}{2}\,\mathrm{e}^{-\mathrm{i}\varphi_n} \quad \times \quad & \left[\int_0^\infty \mathrm{d}x\,x^{n+1}\,w(x)\left(\frac{f_n'(x)}{x}-n^2\frac{f_n(x)}{x^2}-f_n''(x)\right)\right. \\ & \left. -\ 2\int_0^\infty \mathrm{d}x\,\left(\frac{\mathrm{d}\left[x^{n+2}\,w(x)\right]}{\mathrm{d}x}-2x^{n+1}\,w(x)\right)\left(\frac{f_n'(x)}{x}-\frac{f_n(x)}{x^2}\right)\right]\ . \end{aligned} \tag{A5}$$

Integrating the first term of the second integral in (A5) by parts and collecting terms, one immediately sees that (A5) equals (A4), or that $Q^{(n)}_\varphi = Q^{(n)}$. Similarly, from (17), one has

$$Q^{(n)}_x = \frac{\pi}{2}\,\mathrm{e}^{-\mathrm{i}\varphi_n}\left[\int_0^\infty \mathrm{d}x\,\left[2W(x)-x^{n+1}\,w(x)\right]\left(\frac{f_n'(x)}{x}-n^2\frac{f_n(x)}{x^2}-f_n''(x)\right)+2n^2\int_0^\infty \mathrm{d}x\,W(x)\left(\frac{f_n'(x)}{x}-\frac{f_n(x)}{x^2}\right)\right]\ . \tag{A6}$$

Integrating by parts, using (16), and ordering terms yields that (A6) also agrees with (A4), i.e., $Q^{(n)}_x = Q^{(n)}$.

APPENDIX B: INFLUENCE OF MATTER INSIDE AND OUTSIDE THE ANNULUS

We show here how the shear in the annulus $\nu R \le |\vec{x}| \le R$ is affected by matter inside and outside the annulus. In terms of the surface mass density, the shear is given by

$$\gamma(\vec{x}) = \frac{1}{\pi}\int \mathrm{d}^2y\,\mathcal{D}(\vec{x}-\vec{y})\,\kappa(\vec{y}) \quad \text{with} \quad \mathcal{D}(\vec{z}) = \frac{-1}{(Z^*)^2}\ , \tag{B1}$$

where complex notation was used, $Z = z_1 + \mathrm{i}z_2$. For a point $\vec{x}$ in the annulus, $\nu R \le |\vec{x}| \le R$, we then define the *inner* and the *outer* shear by

$$\gamma_{\rm in}(\vec{x}) = \frac{-1}{\pi}\int_0^{\nu R}\mathrm{d}y\,y\int_0^{2\pi}\mathrm{d}\vartheta\frac{\kappa(\vec{y})}{(X^*-y\mathrm{e}^{-\mathrm{i}\vartheta})^2}\quad ,\quad \gamma_{\rm out}(\vec{x}) = \frac{-1}{\pi}\int_R^{\infty}\mathrm{d}y\,y\int_0^{2\pi}\mathrm{d}\vartheta\frac{\kappa(\vec{y})}{(X^*-y\mathrm{e}^{-\mathrm{i}\vartheta})^2}\ . \tag{B2}$$

The calculation is performed by first decomposing κ in Fourier modes,

$$\kappa(\vec{y}) = \sum_{n=0}^{\infty}\kappa_n(y)\,\cos(n\vartheta+\vartheta_n)\ , \tag{B3}$$

and then inserting this expression into (B2). The resulting ϑ-integrals are evaluated by transforming the integration variable to $u = \mathrm{e}^{\mathrm{i}\vartheta}$, $\mathrm{d}\vartheta = -\mathrm{i}\,\mathrm{d}u/u$, and using the residue theorem. For the inner and outer shear, we thus obtain

$$\begin{aligned} \gamma_{\rm in}(\vec{x}) = & -\ \frac{2}{(X^*)^2}\int_0^{\nu R}\mathrm{d}y\,y\,\kappa_0(y) - \sum_{n=1}^{\infty}\frac{(n+1)\,\mathrm{e}^{\mathrm{i}\vartheta_n}}{(X^*)^{(n+2)}}\int_0^{\nu R}\mathrm{d}y\,y^{(n+1)}\,\kappa_n(y)\ , \\ \gamma_{\rm out}(\vec{x}) = & -\ \sum_{n=2}^{\infty}\mathrm{e}^{-\mathrm{i}\vartheta_n}(n-1)\,(X^*)^{(n-2)}\int_R^\infty \mathrm{d}y\,y^{(1-n)}\,\kappa_n(y)\ . \end{aligned} \tag{B4}$$

Defining then the *inner* and *outer* multipole moments analogously by

$$\begin{aligned} Q^{(n)}_{\rm in} &:= \int_0^{\nu R}\mathrm{d}y\,y^{(n+1)}\int_0^{2\pi}\mathrm{d}\vartheta\,\mathrm{e}^{n\mathrm{i}\vartheta}\,\kappa(\vec{y}) = \pi\mathrm{e}^{-\mathrm{i}\vartheta_n}\int_0^{\nu R}\mathrm{d}y\,y^{(n+1)}\,\kappa_n(y)\ , \\ Q^{(n)}_{\rm out} &:= \int_R^{\infty}\mathrm{d}y\,y^{(1-n)}\int_0^{2\pi}\mathrm{d}\vartheta\,\mathrm{e}^{n\mathrm{i}\vartheta}\,\kappa(\vec{y}) = \pi\mathrm{e}^{-\mathrm{i}\vartheta_n}\int_R^{\infty}\mathrm{d}y\,y^{(1-n)}\,\kappa_n(y)\ , \end{aligned} \tag{B5}$$

we can write the inner and the outer shear as

$$\gamma^*_{\rm in}(\vec{x}) = -\frac{1}{\pi}\left(\frac{2Q^{(n)}_{\rm in}}{X^2}\right)+\sum_{n=1}^{\infty}\frac{(n+1)Q^{(n)}_{\rm in}}{X^{(n+2)}}\quad ,\quad \gamma_{\rm out}(\vec{x}) = -\frac{1}{\pi}\sum_{n=2}^{\infty}(n-1)\ (X^*)^{(n-2)}\ Q^{(n)}_{\rm out}\ . \tag{B6}$$

We thus see that the shear in the annulus caused by the matter outside the annulus is fully described by the multipole moments of this matter distribution. The shear is affected by all multipoles of the matter inside the annulus, but only affected by the quadrupole and higher-order terms outside the annulus. In particular, the outer quadrupole moment causes a constant shear over the annulus.

APPENDIX C: APERTURE MASSES FOR ARBITRARY APERTURE SHAPES

We show here that the aperture mass measure (19) can be generalized to apertures of arbitrary shape (in fact, also the aperture multipoles can be generalized, but they will probably be of less use). As before, we define the aperture mass as

$$m(\vec{x}_0) = \int \mathrm{d}^2 y \, w(\vec{y} - \vec{x}_0) \, \kappa(\vec{y}) \; , \tag{C1}$$

where w is a weight function.

C1 Self-similar curves

Let the weight function be constant on self-similar concentric curves. Then define a new coordinate system by choosing a closed curve $\vec{c}(\lambda)$, $\lambda \in I$, and setting

$$\vec{y} = \vec{x}_0 + b\vec{c}(\lambda) \; ; \tag{C2}$$

then the mapping between $\vec{y}$ and (b, λ) is one-to-one (except at $b = 0$) iff $\vec{c} \times \dot{\vec{c}} \neq 0$ for all $\lambda \in I$, where $\vec{c} \times \dot{\vec{c}} = c_1 \dot{c}_2 - \dot{c}_1 c_2$. Without loss of generality, choose $\vec{c} \times \dot{\vec{c}} \geq 0$. The Jacobian of the coordinate transformation is $J = \det[\partial(y_1, y_2)/\partial(b, \lambda)] = b \, \vec{c} \times \dot{\vec{c}}$, and so, if w depends on b only, we find from (C1) that

$$m(\vec{x}_0) = \int_0^\infty \mathrm{d}b \, b \, w(b) \oint_I \mathrm{d}\lambda \left(\vec{c} \times \dot{\vec{c}} \right) \; \kappa \left(\vec{x}_0 + b\vec{c}(\lambda) \right) \; . \tag{C3}$$

We now apply the same strategy that was used for deriving Q_x in the main text. Integrating (C3) by parts with respect to b yields

$$m(\vec{x}_0) = - \int_0^\infty \mathrm{d}b \, b \, W(b) \oint_I \mathrm{d}\lambda \left(\vec{c} \times \dot{\vec{c}} \right) \; \frac{\partial \kappa}{\partial b} \left(\vec{x}_0 + b\vec{c}(\lambda) \right) \; , \tag{C4}$$

where we have defined

$$W(b) := \frac{1}{b} \int_0^b \mathrm{d}b' \; b' \, w(b') \; . \tag{C5}$$

We have further assumed that

$$\int_0^\infty \mathrm{d}b \, b \, w(b) = 0 \tag{C6}$$

to ensure that boundary terms vanish. The partial derivative $\partial\kappa/\partial b$ can now be transformed to

$$\begin{aligned} \frac{\partial \kappa}{\partial b} &= c_1 \frac{\partial \kappa}{\partial y_1} + c_2 \frac{\partial \kappa}{\partial y_2} = c_1 \left(\frac{\partial \gamma_1}{\partial y_1} + \frac{\partial \gamma_2}{\partial y_2} \right) + c_2 \left(\frac{\partial \gamma_2}{\partial y_1} - \frac{\partial \gamma_1}{\partial y_2} \right) \\ &= \frac{1}{\vec{c} \times \dot{\vec{c}}} \left[\left(c_1 \dot{c}_2 + \dot{c}_1 c_2 \right) \frac{\partial \gamma_1}{\partial b} + \left(\dot{c}_2 c_2 - \dot{c}_1 c_1 \right) \frac{\partial \gamma_2}{\partial b} \right] + \frac{1}{b \, \vec{c} \times \dot{\vec{c}}} \left[-2 c_1 c_2 \frac{\partial \gamma_1}{\partial \lambda} + \left(c_1^2 - c_2^2 \right) \frac{\partial \gamma_2}{\partial \lambda} \right] \; . \end{aligned} \tag{C7}$$

After inserting (C7) into (C4), the terms containing partial derivatives with respect to b and λ are integrated by parts with respect to the respective coordinate, making use of (C6). After collecting terms, this yields

$$m(\vec{x}_0) = \int_0^\infty \mathrm{d}b \; \left[2W(b) - b w(b) \right] \oint_I \mathrm{d}\lambda \left[- \left(c_1 \dot{c}_2 + \dot{c}_1 c_2 \right) \gamma_1 + \left(c_1 \dot{c}_1 - c_2 \dot{c}_2 \right) \gamma_2 \right] \; , \tag{C8}$$

hence the aperture mass m can be expressed directly in terms of γ. This result can be written in a more compact form by defining the function

$$q(b) := 2bW(b) - b^2 w(b) = 2 \int_0^b \mathrm{d}b' \, b' \, w(b) - b^2 w(b) \; , \tag{C9}$$

and introducing complex notation, $C(\lambda) = c_1(\lambda) + \mathrm{i} c_2(\lambda)$. This yields

$$m(\vec{x}_0) = \int \mathrm{d}^2 y \; \frac{q(b(\vec{y}))}{b^2(\vec{y})} \, \frac{\Im \left(\gamma(\vec{y}) C^* \dot{C}^* \right)}{\Im \left(C^* \dot{C} \right)} \; , \tag{C10}$$

where C has to be taken at $\lambda(\vec{y})$. This generalizes the aperture mass measure as originally derived by Kaiser (1995), Kaiser et al. (1994) and Schneider (1996b); the generalization to non-circular apertures was first done in Squires & Kaiser (1996). As for circular apertures, choosing $w(b) = \text{const.}$ for $0 \le b \le \nu B$ implies $q(b) = 0$ for this interval, so that the mass inside the curve $b = \nu B$ can be measured from the shear around that region.

C2 Arbitrary curves

We now assume that $w(\vec{x})$ is constant on a set of nested curves of arbitrary shapes; in particular, these curves do not have to be self-similar. In analogy to (C2), we define a new coordinate system by

$$\vec{y} = \vec{x}_0 + \hat{\vec{c}}\left(\hat{b}, \hat{\lambda}\right) \ , \tag{C11}$$

where $\hat{\lambda}$ is a cyclic coordinate, $\hat{\lambda} \in I = [0, \lambda_{\max}]$, and we assume that w depends only on $\hat{b}$. In order for (C11) to define a new coordinate system, we require that the Jacobian

$$\hat{J}(\hat{b}, \hat{\lambda}) = \frac{\partial \hat{\vec{c}}}{\partial \hat{b}} \times \frac{\partial \hat{\vec{c}}}{\partial \hat{\lambda}} \tag{C12}$$

is nonzero everywhere (except at the origin). Without loss of generality, we take $\hat{J} > 0$. The curves will now be relabeled and reparameterized as follows. Let

$$\mathcal{A}(\hat{b}) = \frac{1}{2} \oint \mathrm{d}\hat{\lambda}\, \hat{\vec{c}} \times \frac{\partial \hat{\vec{c}}}{\partial \hat{\lambda}} \tag{C13}$$

be the area enclosed by the curve labeled with $\hat{b}$; then we define a new 'radial' coordinate $b(\hat{b})$ through

$$b = \sqrt{\frac{2\mathcal{A}(\hat{b})}{\lambda_{\max}}} \ , \tag{C14}$$

so that

$$\frac{\mathrm{d}b}{\mathrm{d}\hat{b}} = \frac{1}{\sqrt{2\lambda_{\max}\mathcal{A}(\hat{b})}} \oint \mathrm{d}\hat{\lambda}\, \hat{J}\left(\hat{b}, \hat{\lambda}\right) \ . \tag{C15}$$

We define a new cyclic parameter $\lambda\left(b, \hat{\lambda}\right) \in I$ by requiring that the Jacobian of the new transformation be independent of λ; in particular, the definition of b allows to set the new Jacobian equal to b. Thus, let $\vec{c}(b, \lambda) = \hat{\vec{c}}\left(\hat{b}(b), \hat{\lambda}(b, \lambda)\right)$, then

$$J(b, \lambda) = \vec{c}\,' \times \dot{\vec{c}} = \left[\frac{\mathrm{d}\hat{b}}{\mathrm{d}b}\frac{\partial \hat{\vec{c}}}{\partial \hat{b}} + \frac{\partial \hat{\lambda}}{\partial b}\frac{\partial \hat{\vec{c}}}{\partial \hat{\lambda}}\right] \times \frac{\partial \hat{\lambda}}{\partial \lambda}\frac{\partial \hat{\vec{c}}}{\partial \hat{\lambda}} = \frac{\mathrm{d}\hat{b}}{\mathrm{d}b}\frac{\partial \hat{\lambda}}{\partial \lambda}\hat{J}\left(\hat{b}, \hat{\lambda}\right) = b \ , \tag{C16}$$

where here and in the following, a prime (dot) denotes partial derivatives with respect to b (λ). Equation (C16) determines λ: using (C14) and (C15), we find

$$\lambda(b, \hat{\lambda}) = \frac{\lambda_{\max}}{\oint \mathrm{d}\hat{\lambda}\, \hat{J}\left(\hat{b}(b), \hat{\lambda}\right)} \int_0^{\hat{\lambda}} \mathrm{d}\tilde{\lambda}\, \hat{J}\left(\hat{b}(b), \tilde{\lambda}\right) \ . \tag{C17}$$

These definitions of the new coordinates uniquely define at every point $\vec{y}$ the two vector fields $\vec{c}\,'$ and $\dot{\vec{c}}$. We now proceed as in Sect. C1 before. (C1) is transformed into an integral over the new coordinates (b, λ), and then integrated by parts with respect to b,

$$m(\vec{x}_0) = -\int_0^\infty \mathrm{d}b\, b\, W(b) \oint_I \mathrm{d}\lambda\, \frac{\partial \kappa}{\partial b}\left(\vec{x}_0 + \vec{c}(b, \lambda)\right) \ , \tag{C18}$$

with $W(b)$ defined as in (C5), and the condition (C6) is applied to $w(b)$. The derivative of κ is expressed in terms of derivatives of the shear, using the coordinate transform and (10) to obtain

$$\frac{\partial \kappa}{\partial b} = \frac{1}{b}\left(\Im(C'\dot{C})\frac{\partial \gamma_1}{\partial b} - \Re(C'\dot{C})\frac{\partial \gamma_2}{\partial b} - \Im(C'^2)\frac{\partial \gamma_1}{\partial \lambda} + \Re(C'^2)\frac{\partial \gamma_2}{\partial \lambda}\right) \ , \tag{C19}$$

where complex notation was used again, $C' = c_1' + \mathrm{i}c_2'$. Inserting (C19) into (C18), one obtains after another partial integration

$$m(\vec{x}_0) = \int \mathrm{d}^2y \left\{ \left(\frac{W(b)}{b^2} - \frac{w(b)}{b}\right) \Im\left[\left(C'\dot{C}\right)^* \gamma\right] + \frac{W(b)}{b} \Im\left[\left(C'\dot{C}' - C''\dot{C}\right)^* \gamma\right] \right\} \ . \tag{C20}$$

We note that if one specializes $\vec{c}(b, \lambda) = b\vec{k}(\lambda)$ to self-similar curves, (C20) reduces to (C10) (note that (C16) implies that $\vec{k} \times \dot{\vec{k}} = 1$). If the weight function is chosen to be constant within a curve $b_0\vec{k}(\lambda)$, one can select the family of curves such that $\vec{c}(b\lambda) = b\vec{k}(\lambda)$ for $b \le b_0$, whereas the curves are arbitrary for $b > b_0$ (except of course that the family of curves is twice differentiable). Then, the aperture mass (C1) can be calculated from the shear outside the curve labeled by b_0. One could, for example, generalize the ζ-statistics introduced by Kaiser (1995) to an annular region, where the inner boundary is a circle (e.g., situated on the cluster center), and the outer boundary is the boundary of the CCD. One can easily write down a family of curves which are circles for $b < b_0$, and which smoothly deform into a square for $b = B$. The only difference to the standard ζ-statistics is that the vector fields $\vec{c}\,'$ and $\dot{\vec{c}}$ have to be calculated numerically.

ACKNOWLEDGEMENTS

We thank Matthias Steinmetz for numerically simulating the cluster models used, and Simon White for useful comments. This work was supported in part by the Sonderforschungsbereich SFB 375-95 of the Deutsche Forschungsgemeinschaft.

REFERENCES

Bartelmann, M., & Steinmetz, M. 1996, MNRAS, in press; preprint astro-ph/9603101
Bartelmann, M., Ehlers, J., & Schneider, P. 1994, A&A, 280, 351
Bartelmann, M., Narayan, R., Seitz, S., & Schneider, P. 1996, ApJ, 464, L115
Kaiser, N. 1995, ApJ, 493, L1
Kaiser, N., & Squires, G. 1993, ApJ, 404, 441
Kaiser, N., Squires, G., Fahlman, G., & Woods, D. 1994, in: *Clusters of Galaxies*, eds. F. Durret, A. Mazure, & J. Trân Thanh Vân (Gif-Sur-Yvette: Editions Frontieres)
Richstone, D., Loeb, A., & Turner, E.L. 1992, ApJ, 393, 477
Schneider, P. 1996a, Proc. Laredo Advanced Summer School 1995, in press; preprint astro-ph/9512047
Schneider, P. 1996b, MNRAS, in press; preprint astro-ph/9601039
Schneider, P., Ehlers, J., & Falco, E.E. 1992, *Gravitational Lenses* (Heidelberg: Springer Verlag)
Seitz, C., & Schneider, P. 1995, A&A, 297, 287
Squires, G., & Kaiser, N. 1996; preprint astro-ph/9512094
Wilson, G., Cole, S., & Frenk, C.S. 1996, MNRAS, submitted; preprint astro-ph/9601110